HHS Public Access

Author manuscript

Sci Transl Med. Author manuscript; available in PMC 2021 June 09.

Published in final edited form as:

Sci Transl Med. 2020 December 09; 12(573): . doi:10.1126/scitranslmed.abc5926.

Agonist-antagonist myoneural interface amputation preserves proprioceptive sensorimotor neurophysiology in lower limbs

Shriya S. Srinivasan[1,2,3,*], **Greta Tuckute**[2], **Jasmine Zou**[2], **Samantha Gutierrez-Arango**[2,3], **Hyungeun Song**[1,2,3], **Robert L. Barry**[1,3,4,†], **Hugh M. Herr**[2,*,†]

[1]Harvard-MIT Program in Health Sciences and Technology, Massachusetts Institute of Technology, Cambridge, Massachusetts, USA, 02139

[2]MIT Center for Extreme Bionics, Massachusetts Institute of Technology, Cambridge, Massachusetts, USA, 02139

[3]Athinoula A. Martinos Center for Biomedical Imaging, Department of Radiology, Massachusetts General Hospital, Charlestown, Massachusetts, USA, 02129

[4]Department of Radiology, Harvard Medical School, Boston, Massachusetts, USA, 02115

Abstract

The brain undergoes marked changes in function and functional connectivity after limb amputation. Agonist-antagonist myoneural interface (AMI) amputation is a procedure which restores physiological agonist-antagonist muscle relationships responsible for proprioceptive sensory feedback, to enable greater motor control. We compared results from the functional neuroimaging of individuals (n = 29) with AMI amputation, traditional amputation and no amputation. Individuals with traditional amputation demonstrated a significant decrease in proprioceptive activity, measured by activation of Broadman Area 3a (BA3a), whereas functional activation in individuals with AMIs was not significantly different from no amputation controls ($p < 0.05$). The degree of proprioceptive activity in the brain strongly correlated with fascicle activity in the peripheral muscles and performance on motor tasks ($p < 0.05$), supporting the mechanistic basis of the AMI procedure. These results suggest that surgical techniques designed to restore proprioceptive peripheral neuromuscular constructs result in desirable central sensorimotor plasticity.

One Sentence Summary:

Agonist-antagonist myoneural interfaces in lower limb amputation help preserve sensory feedback to the brain.

[*]Corresponding author. shriyas@mit.edu (S.S.S.), hherr@media.mit.edu (H.M.H.).

Author contributions: S.S.S. contributed to the conceptualization, development of methodology, investigation, data collection and analysis and writing. J.Z., G.T., and S.G.-A assisted with data analysis and writing. H.S. assisted with data collection. R.L.B. contributed to data collection, analyses, and assisted with writing. H.M.H contributed to conceptualization, contributed to the methodology, performed project administration, funding acquisition, and assisted with writing.

[†]These authors contributed to this work as co-senior authors.

Data and materials availability: All data associated with the study are present in the main text or the Supplementary Materials.

Introduction

The traditional amputation procedure devotes little attention to the neurological substrates present in peripheral limbs, leading to considerable neuroma pain ((1),(2),(3)), phantom pain[4], maladaptive central plasticity(4). Cutaneous tissues are discarded during amputation, depriving the sensory cortex of critical sensory feedback. Agonist-antagonist muscle pairs, which give rise to signals of force, velocity, and position, are severed, depriving the central nervous system (CNS) of spindle and Golgi tendon organ-based afferent proprioceptive signals(5).

The aforementioned modifications that a traditional amputation imparts on the peripheral nervous system disrupt the normal sensorimotor mechanisms of the CNS. Prior studies have demonstrated that heterotopic sensorimotor regions exhibit decreased functional activation(6) during tasks involving the phantom limb. Specifically, Brodmann area (BA) 3a(7),(8), which receives proprioceptive input, exhibits reduced excitability in persons with traditional amputation(1). Additionally, sensory processing circuits became fragmented, evidenced by a reduction of hemispheric symmetry(9), compensatory effects in the ipsilateral sensorimotor region(10), and decreased functional connectivity (FC) of intra-sensorimotor, sensorimotor-premotor, and supplementary motor-subcortical nuclei(11),(12),(13). To reconcile the discrepancy between efferent motor imagery(14) and the movement of the phantom or prosthetic limb, persons with traditional amputation further develop a dependence on visual stream, as observed through gray matter thickening in visual regions(15) and greater coupling of the visual and default mode networks(16),(17),(18). Together, these CNS changes precipitate inadequate control signal generation for neuroprostheses(19),(20),(21), and maladaptive phantom sensation(22),(23),(24), which greatly lower neuroprosthetic controllability(20),(21) and the quality of life(19),(7),(8),(25).

We posited that strategic reconstruction of neuromusculature during amputation can preserve central sensorimotor mechanisms towards enhanced neuroprosthetic control after amputation. Di Pino *et al.* (26) suggested that such a system which restores native neural connections could drive neuroplastic phenomena towards more ‘desirable plasticity’ – a state devoid of aberrant phantom sensations and phantom pain, resembling the unaffected brain with afferent and efferent signaling. Here, we studied a cohort of persons that have undergone an amputation strategy called the agonist-antagonist myoneural interface (AMI) amputation. AMI amputation is a reconstructive surgery and neural interfacing strategy that engineers residual physiology with a focus on peripheral and central neurological remodeling towards neuroprosthetic control(5, 27–33). During an AMI amputation, agonist-antagonist muscles are coapted, restoring physiological neuromuscular dynamics (Fig. 1). Contraction of the agonist muscle stretches the mechanically-coupled antagonist muscle, or vice versa, giving rise to natural proprioceptive mechanotransduction through spindle fibers and golgi tendon organs. These proprioceptive afferents play an integral role in the loop of sensory perception and motor execution. By restoring proprioceptive neuromuscular constructs, the AMI is designed to promote near-native physiological function of the central-peripheral sensorimotor signaling mechanisms, thus promoting realistic phantom motor imagery and efferent control. Preclinical neurophysiological studies and human trials have shown graded peripheral afferent/efferent signaling and greater efficiency in neuroprosthetic

control tasks and force discrimination(30), but direct evidence of the AMI amputation's proprioceptive capacity and systemic neurophysiological impact have yet to be characterized.

Results

We performed functional neuroimaging of patients with AMI amputation (AA) (n = 12), traditional amputation **(TA)** (n=7) and no amputation **(NA)** (n=10, control) to observe and analyze central nervous system processes. Individuals with TAs and AAs underwent similar rehabilitation and gait training and utilized a passive prosthesis. We assayed peripheral functions, including fascicle dynamics, motor task performance, and phantom sensation (Fig. 1), and used these metrics to investigate the interplay of proprioceptive and motor control mechanisms. We hypothesized that the functional activation of the proprioceptive center (BA3a) in the brain will be (i) undiminished in individuals with AAs as compared to NAs, (ii) correlated with muscle spindle activity and (iii) correlated to motor control performance on tasks requiring proprioception. We also hypothesized that individuals with AAs would present with heightened connectivity of sensorimotor areas. As an exploratory investigation, we probed whole-brain functional connectivities in task and resting state.

Functional activation in BA3a

The AMI amputation is specifically designed to preserve the agonist-antagonist muscle relationships that enable spindle fiber and Golgi tendon organ-based proprioceptive afferents, which are decoupled in traditional amputation. In the brain, proprioception is measured by BA3a(7),(8) activation and contributes to limb positioning(19). Here, individuals performed the task of dorsiflexing and plantarflexing their ankle or phantom ankle. Blood oxygenation level dependent (BOLD) responses within heterotopic leg regions for each BA were quantified (Fig. 2, A and B) and group comparisons were evaluated with nonparametric Kruskal-Wallis H tests using a threshold of $P < 0.05$. The BA3a region of interest (ROI) was activated to a lesser degree in TAs (0.09% +/− 0.47%) than NAs (0.83 +/− 0.46%, $P < 0.005$). However, AAs (0.83% +/− 0.39%) activated BA3a to a similar extent as NAs ($P < 0.7$). No significant differences were found in the hemisphere ipsilateral to the affected leg in the BA3 and BA4 areas (Fig. S1).

The fundamental physiological relationship between spindle stretch and proprioceptive afferents was assayed by comparing the mean fascicle strains (correlated to spindle fiber activity) of each individual to his/her BOLD activity in BA3a (Fig. 2C). A strong correlation ($r = 0.70$, $P < 0.05$) was present and revealed significantly distinct clusters between AA and TA groups (F-statistic = 4.39, $P < 0.002$, nonparametric multivariate analysis of variance). Further, individuals performed a position differentiation task moving their phantom joints to specified locations – an indicator of proprioception, motor control and neuroprosthetic controllability. The precision of muscle activation using electromyographic (EMG) signals from AMI muscles was quantified to evaluate performance (on a scale from 0 to 2). Performance on the position differentiation task correlated linearly ($r = 0.64$, $P < 0.01$) with the functional activation of BA3a, with distinct separation of the TA and AA groups (Fig. 2D, F-statistic = 6.99, $P < 0.02$, nonparametric multivariate analysis of variance). Overall,

these data demonstrate that the activation of the BA3a region in AAs is not only similar to NAs, but is also correlated strongly with muscle excursion and motor control, supporting the mechanistic underpinnings of the AMI.

Functional sensorimotor connectivity and phantom sensation

To investigate the effect of functional plasticity on coactivation within the sensorimotor cortices, we assayed the FC within the motor (M1) and somatosensory (S1) regions consisting of BA3a, 3b, 4a, and 4p regions, responsible for sensory feedback, primary sensory function, motor execution and motor initiation, respectively(34). The average FC between each region is denoted in the matrices in Fig. 3A. The average connectivity within the sensorimotor cortex for AAs was significantly higher than the NAs and TAs ($p < 0.05$, nonparametric Kruskal-Wallis test with Bonferroni correction). FCs between all BA regions were lower for TAs as compared to NAs, except for BA3a-BA3b and BA3b-BA4p.

An analysis of brain-wide ROI-to-ROI FC of anatomical seeds during task was performed to identify the connections that were significantly modified by traditional and/or AMI amputation ($p^{FDR} < 0.05$) (Fig. 3, B and C). Effect sizes for each are presented in fig. S2. Post-hoc analyses enabled the parsing of group-wise trends to reveal the connections that were significantly strengthened or weakened with amputation (nonparametric ANOVA). The medial frontal cortex showed greater connectivity to various regions in AAs compared to TAs or BCs.

Phantom sensation is an indicator of the brain's representation of the body and is linked to neuroplastic changes in FC(35),(36). With greater deafferentation, there is generally a greater loss of phantom sensation and studies have demonstrated a shift in FC in patients with and without phantom sensation. However, the relationship between the degree of phantom sensation and connectivity changes has not been investigated(11).We thus analyzed connectivities amongst anatomical and network seeds in relationship to the phantom sensation score reported by each individual during the resting and task scans (Fig. 3, D and G). We corrected for multiple comparisons using the Benjamin-Hochberg method and assessed significant relationships based on a new alpha (0.35) at the fifth percentile of adjusted P values (see fig S3). During the task state, operculum area 4 (OP4) to BA6d2 precentral gyrus (PreCG) connectivity strongly correlated with stronger phantom sensation ($r = 0.71$, $P < 0.002$) (Fig. 3E). Further, connectivities between the cerebral dorsal dentate and the BA3a, BA3b ($r = 0.76$, $P < 0.009$), and BA4a correlated strongly with phantom sensation. During resting state, connectivity between the visual and sensorimotor networks were strongly coupled for individuals with weaker phantom sensation. The majority of AAs had phantom sensation scores greater than 6/10 and demonstrated lower coupling of the visual and sensorimotor networks when compared to the TAs. The strongest negative correlation was seen for the visual occipital and superior sensorimotor networks (Fig. 3H, $r = 0.64$, $P < 0.011$). Scatterplots of the five most positively and negatively correlated regions are provided in figs. S4 and S5.

Discussion

Here we found that the AMI amputation's strategic reconstruction of the peripheral neuromusculature has a measurable neuroplastic effect in reengaging sensory feedback and motor imagery functionality. Specifically, the AMI amputation promotes proprioceptive feedback, functional connectivity, and potentially decreases visuomotor dependence as compared to persons with a traditional amputation.

TAs demonstrated a decrease in the BA3a activation, consistent with prior studies(6). AAs activated the BA3a region similarly to NAs, demonstrating the AMI's capacity to facilitate physiological proprioceptive feedback for plantar and dorsiflexion tasks. Greater fascicle strains were predictive of greater BA3a BOLD response, which is corroborated by the operating principles of spindle-fiber mechanotransducers(37) and preclinical neurophysiological investigations of AMIs(5, 29, 31). As witnessed previously in stroke patients(38),(39), BA3a activity is linked to motor imagery ability and trends with enhanced motor performance. Similarly, individuals with AMIs' performance on tasks requiring motor control and proprioception was greater than TAs, as evidenced by the position differentiation task scores in this study as well as prosthetic controllability tasks previously published(30). Conceivably, the afferent feedback after AMI amputation may contribute to the augmented motor performance.

Connectivity analyses further shed light on the effect of the AMI amputation on brain regions involved with motor coordination and correction. Previous studies in animal deafferentiation models(40) and humans with traditional amputation(11) have shown decreased FC between intra- and inter-sensorimotor regions. As compared to NAs and TAs, in AAs the medial frontal cortex showed increased connectivity to several regions, including the frontoparietal areas. The medial frontal cortex plays a role in error correction, motion performance, and spatial judgement(41, 42). The frontoparietal region incorporates circuitry between motor imagery and motor execution and may be involved with feedback loops for attention devoted to motor control(24). Frontoparietal lesions have been shown to result in impaired motor imagery(43) and mental chronometry tasks(44),(45), both functions invoked during the task studied here. The heightened connection of these regions may correspond, at least in part, to the changes evoked by AMI amputation and their peripheral limb functionality. Although FC was lower in TAs for most sensorimotor regions, there was no significant difference in BA3a-BA3b and BA3b-BA4p. Further investigation will be required to ascertain the underpinning reason.

The assay of connectivities with degree of phantom sensation provided insight as to the areas of the brain associated with heightened motor imagery and planning capabilities after deafferentiation of the homotopic joint. Opercular connectivity (OP4) with the BA6 region was strongly correlated to a greater degree of phantom sensation. The operculum relays sensory feedback for motor actions(24) and the primary responsibility of BA6 is sensory integration. Lesions in BA6 result in apraxi and difficulty in using sensory feedback in a motor control loop(46). As studied in spinocerebellar ataxia type 2(47), stroke(48), and multiple sclerosis(49), BA6 supplementary motor area (SMA) connectivity also positively correlates with motor function. Given these functions, greater phantom sensation production, as seen in AAs, aligns with increased coactivation of sensory feedback areas.

Persons with traditional amputation rely heavily on their visual stream to provide information regarding the position and velocity of their prosthetic limbs because there is no sensory feedback from the prosthesis or limb itself(24). In line with this behavior, prior studies have demonstrated a compensatory coupling of the visual system to the sensorimotor system in the brain of persons with traditional amputation(17),(50). Our connectivity analysis during the resting state scan demonstrated decreased coupling of the visual and sensorimotor networks for individuals with greater phantom sensations, with the majority of AAs clustered in the region with low connectivity and higher phantom sensation. We speculate that the presence of physiological afferents in individuals with AMIs may promote healthy motor imagery and reduce their dependence on the visual streams. Prior studies have indicated that enhanced phantom sensations improve a sense of agency and improve motor control performance(51, 52) as they provide a more reliable and actionable map of motor imagery. Although these were largely performed in individuals with upper extremity amputation, we posit that the principle translates to individuals with lower extremity amputation as well.

In the future, a larger set of participants should be included and reconstructive strategies incorporating cutaneous sensory feedback should be investigated, considering the critical role of cutaneous sensation in guiding movement. Functional activation of other areas involved in proprioception, such as subcortical nuclei, should be explored. In this study, the effect on central plasticity of traditional versus AMI amputation was investigated without consideration of neural prosthetic training influences that may promote optimal central plasticity. In future studies, conducting neuroimaging before and after a period of external neural prosthetic training may serve as an important exploration of motor memory and sensorimotor preservation for persons with limb amputation. Further, the effect of this amputation methodology on phantom pain would yield valuable scientific insight with clinical relevance, and should be a focus of future studies. These studies may even be leveraged to develop and implement specialized rehabilitation protocols for to promote the optimal central plasticity.

Instead of viewing amputation as a failure of limb salvage treatment, we urge the neuroscience and surgical communities to conceptualize amputation as a reconstructive procedure that can functionalize the amputated limb and sculpt peripheral and central neural substrates(53). Strategically rewiring peripheral neural substrates can promote neuroplastic restoration to baseline, increasing sensory feedback and motor capabilities towards improved neuroprosthetic capability.

Methods

Study design

Unilateral transtibial AMI amputees (AA) (n=12), traditional amputees (TA) (n=7), and biologically intact controls (NA) (n=10) were recruited and consented under Massachusetts General Hospital Institutional Review Board protocol #2017P002635 in a non-blinded fashion. Patients in each cohort underwent anatomical and functional neuroimaging while performing a simple movement task. Analysis of the resulting data was used to answer

hypotheses regarding the extent of neuroplastic modifications in relation to proprioceptive feedback from the peripheral limbs.

Patients were matched through a yoked review prioritizing age and time since amputation. Our matching criteria were developed based on prior studies investigating sensorimotor plasticity after surgery(22),(15),(16),(54). These prioritized age (±7 years of difference between matches, SD 4.16 years) and time from amputation to scan date (±13 months of difference between matches, SD ±6.15 months). Although prior studies matched individuals with a tolerance of up to 32 years in terms of age(54, 55) and 40+ years in terms of amputation to scan date(56, 57), we used 7 years and 30 months as our thresholds, respectively. All individuals met the following inclusion criteria: (i) aged 18 or older, (ii) English as a primary language, (iii) no neurological or psychological conditions, (iv) no claustrophobia, (v) no presence of implanted medical hardware, and (vi) willingness to complete an magnetic resonance imaging (MRI) scan. Written informed consent was obtained from all participants prior to imaging. Participant demographics, amputated limb, dominant side, gender, age at amputation, time between amputation and the scan are summarized in table S1.

The participants in the AMI amputation group were recruited through the Brigham and Women's Hospital approved IRB protocol #A-20460. Individuals with AMI underwent an amputation paradigm which created agonist-antagonist myoneural interfaces (AMIs) for the subtalar and ankle joints(30, 32). The ankle AMI was constructed by mechanically linking the lateral gastrocneumius to the tibialus anterior muscle. Further, the subtalar AMI was constructed by linking the tibialis posterior and the peroneus longus muscle. In each AMI, each muscle was mechanically linked to its partner via a tendon, which passed through a synovial canal, harvested from the amputated ankle joint at the time of amputation. Through dynamic coupled motion, the agonist and antagonist AMI muscles generate afferent feedback, reflecting proprioceptive sensations of joint position, speed and torque from advanced limb prostheses(32),(30). Individuals with TA were recruited through (i) advertisements placed in Boston area hospitals, rehabilitation centers, and prosthetics facilities and a (ii) research patient data registry facilitated by the Partners Healthcare System. Individuals with TA underwent standard amputation in hospitals located in the northeast region of the United States.

The AA and TA groups were scanned at least 6 months after the amputation procedure, when primary healing and recovery were complete. For individuals with AMI, appropriate postoperative recovery and dynamic functioning of the AMI constructs was also ensured. Participants reported no acute pain at the time of the scan and demonstrated the ability for ambulation at variable cadence. No individuals used active or neural prostheses at or before the time of the study. All surveyed participants used prostheses for upwards of 11 hours seven days a week.

Data acquisition

Whole-brain structural and functional MRI data were collected at the Athinoula A. Martinos Center for Biomedical Imaging, Department of Radiology, Massachusetts General Hospital using the "Connectome" scanner, based upon a Siemens Skyra 3T, with custom Gmax = 300

mT/m “connectom” gradients and 200 T/m/s slew rate. Inside the custom 64-channel array coil(58), head motion was restricted by foam padding. Participants were positioned in a supine position with a pillow placed under their knees to minimize spontaneous or task-related motion. Anatomical data were acquired using a T1-weighted magnetization-prepared rapid acquisition gradient echo sequence (MPRAGE) with 1-mm isotropic resolution (208 slices, flip angle = 7°, repetition time (TR) = 2530 ms, echo time (TE) = 1.61 ms, GeneRalized Autocalibrating Partial Parallel Acquisition (GRAPPA) factor = 4, acquisition time = 3 min 40 sec).

Resting-state fMRI

Particpants were imaged during an 8-minute resting-state period (2-mm isotropic voxels, 68 slices, flip angle = 41°, TR = 1080 ms, TE = 30 ms).

Task-based fMRI

Visual instructions using Psychtoolbox-3.0.14 were projected onto a screen located at the end of the scanner bore towards the participant’s head. The mirror reflecting movement commands was angled away from the lower extremities, preventing any visual feedback of the leg to the participant. Individuals were first instructed to perform small ankle movements to approximately 25% of their full range of motion. This data was used to localize the region producing the motor efferent commands for the ankle. Then, participants were instructed to alternate between plantarflexion and dorsiflexion of their ankle or phantom ankle to 75% of the full ankle range of motion at a 1 Hz frequency for 20 seconds (18 dynamic volumes). Three repetitions of this task were performed within each run, with 30 seconds of baseline (no activity) between tasks (2-mm isotropic voxels, 68 slices, flip angle = 41°, TR = 1080 ms, TE = 30 ms, GRAPPA factor = 2). Each participant practiced the directed movements prior to scanning, aiming to ensure stable and accurate performance across the localizer and task conditions. TAs and AAs performed actual phantom movements - excursing the appropriate muscles - rather than imagined movements (see (2) for further details). A custom-built pressure bladder system was placed on the tibialis anterior to measure muscle activation during task. Muscle activation produced a superficial bulge, which was measured by the bladders and used to track task performance during the scan. A representative trial is presented in fig S6, showing one repetition of the 25% localizer and 75% ankle movement task. Visual feedback of this pressure reading was utilized to train individuals to activate to the 25% and 75% extents during the practice session. No participants reported difficulty or pain in moving the ankle through the requested ranges of motion. Further, no significant differences were present in their demonstrated ranges of motion, which were mirrored on the contralateral limb ($p < 0.05$, Kruskal Wallis nonparametric test).

Neuroimaging data processing

Custom non-linear gradient corrections were first applied to all data. We then performed two types of data analysis: (i) targeted sensorimotor and (ii) exploratory whole-brain analyses.

Targeted sensorimotor analyses—For the targeted sensorimotor analyses, pre-processing of the structural data included a 3D 3-dimensional rigid-body motion correction to retrospectively compensate for head motion using FreeSurfer (stable version 6.0(59)) as

well as the cortical reconstruction of participants' T1 scans. The processing stream included MNI transformation (MNI152), intensity normalization, skull stripping, volumetric labeling, white matter segmentation, cortical parcellation and projection onto an inflated cortical surface. These inflated surfaces were used for all targeted data analyses. The skull stripping was also reviewed and manually edited for technical accuracy.

Pre-processing of the functional data included motion and slice-timing correction as well as spatial smoothing using a Gaussian filter with a FWHM of 5 mm. Low-frequency signal drift was modelled and removed using a second-order polynomial. To allow statistical comparisons between the right- and left-sided amputees, deafferented hemispheres contralateral and afferented hemispheres ipsilateral to the affected sides were grouped. In the NA group, the ipsilateral hemisphere to their dominant side was compared to the amputees' deafferented hemisphere.

Using FreeSurfer's BA atlas, we generated labels for the sensorimotor regions, including BA 3a, 3b, 4a, 4p, and 6. These labels were customized to include only the 70% most likely vertices in order to minimize overlap amongst these labels.

To identify participant-specific regions of interest (ROI) representing the ankle, we used the BOLD contrast between the baseline condition and the localizing task (25% of range of motion movement). Looking within the dorsomedial wall, the somatotopic location of the lower leg, the vertices that demonstrated a preferential activation ($p < 0.05$) during the localizing task were selected for the ROI. This ankle ROI was then subdivided into its BA 3a, 3b, 4a, and 4p components by taking the intersection of the vertices in our ankle ROI and our predefined BA labels. The mean ROIs are provided in fig S7. No ROI was produced for one individual in the AA group.

BOLD activity was calculated to be the difference between the activation at pre-stimulus baseline and the 75% condition. For one individual in the AA group, the ROI was localized on a vascular substrate, leading to unrealistic BOLD values. This individual was not included in the analyses.

Functional connectivity (FC), or the degree of temporal correlation between spatially distributed signals, has been commonly studied in the context of motor pathologies and amputation as a metric of both central and peripheral coordination. FC serves as a potent metric to evaluate central neuroplasticity in relation to peripheral function as it is predominantly driven by organizational principles, stable individual characteristics, and is relatively immune to day-to-day variability(60). We probed the FC between groups by taking the Pearson correlation of the average BOLD response in our Brodmann-Area constrained functionally-defined ankle ROI during the 75% range of motion task. Brodmann Areas 3a, 3b, 4a and 4p were prioritized in this analysis due to their relavent role in the task.

Exploratory whole-brain connectivity analyses—Many regions beyond the sensorimotor cortex play a role in sensory processing and motor function. To investigate the relevant regions, we performed a whole-brain FC analysis, using a seed-based FC approach. Task-based fMRI data was analyzed using the Functional Connectivity Toolbox (CONN)

version 18.b (Whitfield-Gabrieli & Nieto-Castanon). The fMRI preprocessing steps included functional realignment, slice-timing correction, ART-based outlier identification, coregistration with the structural image in Montreal Neurological Institute 152 (MNI 152) standard space, and spatial smoothing (Gaussian filter with a FWHM of 8 mm) (default pre-processing pipeline). After pre-processing, the residual BOLD signals were filtered with a 0.01 Hz high-pass filter to remove excessive low-frequency drifts and motion-regressed using linear detrending. The results of motion correction and denoising are presented in figs. S8 and S9. Two individuals in the TA group were excluded: one was the aforementioned outlier and the other did not meet quality control standards.

Data collected for individuals with a right-sided amputation were mirror-reversed across the mid-sagittal plane before all analyses so that the “affected” hemisphere was consistently aligned. The hemisphere contralateral to amputation (“affected”) is therefore always displayed as the right hemisphere, while the hemisphere ipsilateral to amputation (“non-affected”) is displayed as the left hemisphere. Data collected for an equal proportion of NAs was also flipped (n=3), in order to account for potential biases stemming from this procedure.

The resulting functional data in MNI space were used for functional connectivity analyses. Regions of interest were derived from the CONN atlas with cortical ROIs from the FSL Harvard-Oxford atlas(61) and the AAL atlas(62),(63). The CONN network ROIs were *a priori* selected from the HCP-ICA project(64) for relevance to the sensorimotor systems. Moreover, cyto- and myelo-architectonic sensorimotor seeds were extracted from the Jülich histological atlas (JuBrain Anatomy Toolbox v3.0)(65).

For each individual, ROI-wise connectivity was measured by extracting the residual time course data from each ROI and calculating the Pearson correlation coefficients between each ROI pair. The correlation coefficients were converted to normally-distributed scores using Fisher’s transform. The resulting ROI-to-ROI connectivity matrices for each individual were entered into a second-level random-effect GLM analysis for statistical comparisons among the three groups. The contrast between groups was set as follows: [AA TA NA][−1 1 0; 0 −1 1; −1 0 1]. Between conditions, contrast parameters were set to compare the activation between 75% ankle movement and the pre-stimulus baseline period.

Assessment of Phantom Sensation, Fascicle Dynamics, and Motor Control

Individuals’ peripheral nervous system outcomes were assessed through testing at the Massachusetts Institute of Technology (MIT) Biomechatronics Lab under MIT IRB Protocol #1609692618. Two individuals with TA who participated in the central neuroimaging were not able to complete this testing at the MIT Biomechatronics lab. Consequently, all data analysis involving both central and peripheral metrics omitted these individuals.

To characterize phantom limb sensation, individuals were asked to describe their phantom limb percepts during walking with a prosthesis, and sitting with and without the prosthesis. For these evaluations, each individual with AA and TA used their take-home passive conventional transtibial prosthesis; a neurally controlled powered prosthesis was not used by either cohort throughout the study. Patients were specifically asked to relate the vividness of

perception of their lateral and medial malleoli, heel pad, arch of the foot, balls of the footpad, and toes. Responses were graded on a 1–3 scale and normalized to yield a phantom sensation score.

In traditional amputation, a myodesis is performed wherein muscles at the end of the residuum are sutured together, resulting in considerable scarring of muscles to one another which prevents their motion. In contrast, muscles comprising the AMI are specifically designed to sliding, contract and stretch to generate afferent spindle-feedback. Since spindle fibers run parallel to muscle fibers, we quantify the muscle fascicle excursion using ultrasound to characterize spindle activity. Individuals were instructed to cycle the phantom ankle joint to various degrees while recording ultrasound from the tibialis anterior using a portable high-definition ultrasound scanner at 60 fps (LS128, Telemed). Fascicles were identified, tracked, and measured using the UltraTrack v2 MATLAB package. The average fascicle strain across at least 10 trials was utilized for all comparisons.

The motor control of the muscles was assessed through the performance of a position differentiation task requiring proprioception. The tibialis anterior, gastrocnemius, peroneus longus, and tibialis posterior muscles were superficially palpated and bipolar surface electrodes were placed on these locations. EMG was acquired using a TMSi Refa 128 Measurement System (Refa_Ext-128e4b4a, REF: 95–0121-6446–0, Sampling Rate: 2048). Wireless goniometers (Bio-Metrics LTD, WS200 DataLITE 2 Goniometer system with W110-Ankle and W150-Knee, and DataLITE Management Software 51025–00) were placed on the ankle and subtalar joints of the unaffected limb. These sensors provided a one-to-one comparison of the intended phantom movements via the mirrored movement of the contralateral limb. Individuals were instructed to move the limb to 0, 25%, 50%, 75% or 100% of the full range of motion for plantarflexion and dorsiflexion. Individuals were instructed to move the subtalar joint to 50% or 100% of the range of motion for inversion and eversion. Commands for each position were presented 20 times and in random order through a custom MATLAB script displayed on an overhead screen. This task's design assays the proprioceptive feedback received and incorporated into one's motor control. Individuals with greater proprioception would be able to better determine the position of the joint and thus more precisely execute the task at each command. For each individual, the difference between the root-mean-squared EMG produced from the target muscles between adjacent positions was computed (i.e.: 0–25, 25–50, 50–75, 75–100), divided by the variance of his/her performance, and normalized to a scale between 0 and 2. An individual executing task with high precision and differentiability between commands would score closer to 2, whereas an individual with worse control would score closer to 0.

Fascicle dynamics, motor control and phantom sensation metrics were evaluated against functional activation in the brain to yield insight regarding peripheral-central neurological remodeling. Individual subject-level data for functional activation and neuromuscular metrics are provided in Table S2.

Statistical analysis

To assess statistical significance for functional neuroimaging during the task, a Kruskal Wallis test was used with an alpha of 0.005. To assess correlations between the position

differentiation task scores or fascicle strain and BOLD signal change percentage in the BA3a region, a multivariate analysis of variance (MANOVA) at an alpha of 0.005 was performed. We probed the statistical significance of FC between groups by utilizing a Pearson correlation of the average BOLD response in our Brodmann-Area constrained functionally-defined ankle ROI during the 75% range of motion task. For the exploratory whole-brain connectivity analysis, statistical maps were evaluated at the seed-level to a false-discovery rate (FDR) of $P < 0.05$ with a two-tailed approach (effect sizes visualized in Fig. S2). Post hoc multivariate ANOVA was used to investigate directionality and significance among all three groups. Statistical analyses for matrices produced comparing the phantom sensation to FC were corrected for multiple comparisons using the Benjamin-Hochberg method. The distribution of the adjusted P values was assessed and a new threshold of alpha = 0.35 was determined at the fifth percentile of the distribution (Fig. S3) for significant relationships.

Supplementary Material

Refer to Web version on PubMed Central for supplementary material.

Acknowledgments:

The authors thank J. Cardona, B. Diamond, E. Israel, M. O'Hara, N. Ohringer, B. Schelhaas, and L. White, for their help recruiting/screening participants and/or conducting scans, Dr. S. Nasr for help setting up the visual stimulus, and Dr. A. Yendiki for help with image reconstruction. We also thank Dr. B. Rosen, Dr. J. Schaechter, and Dr. D. Greve for their valuable insights, discussions, and help with FreeSurfer, respectively. We thank Dr. A. Nieto-Castañón for helpful discussions on analyses using the CONN toolbox.

Funding: This project was supported by funds from the MIT Media Lab Consortia. Imaging was performed at the Athinoula A. Martinos Center for Biomedical Imaging at the Massachusetts General Hospital using resources provided by the Center for Functional Neuroimaging Technologies (P41EB015896) and the Center for Mesoscale Mapping (P41EB030006), Biotechnology Resource Grants supported by the National Institute of Biomedical Imaging and Bioengineering, National Institutes of Health (NIH). The NIH also provided support through grants R00EB016689 and R01EB027779 (R.L.B.). This research was also supported in part by the MGH/HST Athinoula A. Martinos Center for Biomedical Imaging.

Competing interests: S.S.S. and H.M.H. are inventors on patents related to this work: "Peripheral Neural Interface Via Nerve Regeneration to Distal Tissues. # US9474634B2 and "Method And System For Providing Proprioceptive Feedback And Functionality Mitigating Limb Pathology. #US20190021883. All other authors declare no competing interests.

References

1. O'Reilly MAR, O'Reilly PMR, Sheahan JN, Sullivan J, O'Reilly HM, O'Reilly MJ, Neuromas as the cause of pain in the residual limbs of amputees. An ultrasound study, Clinical Radiology 71, 1068.e1–1068.e6 (2016).
2. Makin TR, Scholz J, Filippini N, Slater DH, Tracey I, Johansen-Berg H, Phantom pain is associated with preserved structure and function in the former hand area, Nature Communications 4, 1570 (2013).
3. Flor H, Nikolajsen L, Jensen TS, Phantom limb pain: a case of maladaptive CNS plasticity?, Nat Rev Neurosci 7, 873–881 (2006). [PubMed: 17053811]
4. Molina-Rueda F, Navarro-Fernández C, Cuesta-Gómez A, Alguacil-Diego IM, Molero-Sánchez A, Carratalá-Tejada M, Neuroplasticity Modifications Following a Lower-Limb Amputation: A Systematic Review, PM R (2019), doi:10.1002/pmrj.12167.
5. Srinivasan SS, Carty MJ, Calvaresi PW, Clites TR, Maimon BE, Taylor CR, Zorzos AN, Herr H, On prosthetic control: A regenerative agonist-antagonist myoneural interface, Science Robotics 2, eaan2971 (2017). [PubMed: 33157872]

6. Bruurmijn MLCM, Pereboom IPL, Vansteensel MJ, Raemaekers MAH, Ramsey NF, Preservation of hand movement representation in the sensorimotor areas of amputees, Brain 140, 3166–3178 (2017). [PubMed: 29088322]
7. Razmus M, Daniluk B, Markiewicz P, Phantom limb phenomenon as an example of body image distortion, Current Problems of Psychiatry 18, 153–159 (2017).
8. Ali S, Fatima Haider SK, Psychological Adjustment To Amputation: Variations On The Bases Of Sex, Age And Cause Of Limb Loss, J Ayub Med Coll Abbottabad 29, 303–307 (2017). [PubMed: 28718253]
9. Xie H, Kane JT, Dennis MJ, Mooney RD, Bauer WR, Wang X, Wall JT, Case series evidence for changed interhemispheric relationships in cortical structure in some amputees, J Clin Neurosci 20, 523–526 (2013). [PubMed: 23313520]
10. Mizuguchi N, Nakagawa K, Tazawa Y, Kanosue K, Nakazawa K, Functional plasticity of the ipsilateral primary sensorimotor cortex in an elite long jumper with below-knee amputation, Neuroimage Clin 23 (2019), doi:10.1016/j.nicl.2019.101847.
11. Bramati IE, Rodrigues EC, Simões EL, Melo B, Höfle S, Moll J, Lent R, Tovar-Moll F, Lower limb amputees undergo long-distance plasticity in sensorimotor functional connectivity, Sci Rep 9, 1–10 (2019). [PubMed: 30626917]
12. Zhang J, Zhang Y, Wang L, Sang L, Li L, Li P, Yin X, Qiu M, Brain Functional Connectivity Plasticity Within and Beyond the Sensorimotor Network in Lower-Limb Amputees, Front Hum Neurosci 12, 403 (2018). [PubMed: 30356798]
13. Hernandez-Castillo CR, Diedrichsen J, Aguilar-Castañeda E, Iglesias M, Decoupling between the hand territory and the default mode network after bilateral arm transplantation: four-year follow-up case study, Brain Imaging and Behavior 12, 296–302 (2018). [PubMed: 28185062]
14. Saruco E, Guillot A, Saimpont A, Di Rienzo F, Durand A, Mercier C, Malouin F, Jackson P, Motor imagery ability of patients with lower-limb amputation: exploring the course of rehabilitation effects, Eur J Phys Rehabil Med 55, 634–645 (2019). [PubMed: 29144105]
15. Jiang G, Yin X, Li C, Li L, Zhao L, Evans AC, Jiang T, Wu J, Wang J, The Plasticity of Brain Gray Matter and White Matter following Lower Limb AmputationNeural Plasticity (2015), doi:10.1155/2015/823185.
16. Makin TR, Filippini N, Duff EP, Henderson Slater D, Tracey I, Johansen-Berg H, Network-level reorganisation of functional connectivity following arm amputation, Neuroimage 114, 217–225 (2015). [PubMed: 25776216]
17. Chan AW-Y, Bilger E, Griffin S, Elkis V, Weeks S, Hussey-Anderson L, Pasquina PF, Tsao JW, Baker CI, Visual responsiveness in sensorimotor cortex is increased following amputation and reduced after mirror therapy, Neuroimage Clin 23 (2019), doi:10.1016/j.nicl.2019.101882.
18. Claret CR, Herget GW, Kouba L, Wiest D, Adler J, von Tscharner V, Stieglitz T, Pasluosta C, Neuromuscular adaptations and sensorimotor integration following a unilateral transfemoral amputation, Journal of NeuroEngineering and Rehabilitation 16, 115 (2019). [PubMed: 31521190]
19. van der Schans CP, Geertzen JHB, Schoppen T, Dijkstra PU, Phantom pain and health-related quality of life in lower limb amputees, J Pain Symptom Manage 24, 429–436 (2002). [PubMed: 12505212]
20. Nelson AW, The painful neuroma: the regenerating axon verus the epineural sheath, J. Surg. Res. 23, 215–221 (1977). [PubMed: 886855]
21. Wright J, Macefield VG, van Schaik A, Tapson JC, A Review of Control Strategies in Closed-Loop Neuroprosthetic Systems, Front Neurosci 10 (2016), doi:10.3389/fnins.2016.00312. [PubMed: 26858590]
22. Pazzaglia M, Zantedeschi M, Plasticity and Awareness of Bodily Distortion, Neural Plast 2016 (2016), doi:10.1155/2016/9834340.
23. Collins KL, Russell HG, Schumacher PJ, Robinson-Freeman KE, O'Conor EC, Gibney KD, Yambem O, Dykes RW, Waters RS, Tsao JW, A review of current theories and treatments for phantom limb pain, J Clin Invest 128, 2168–2176.
24. Sharma N, Jones PS, Carpenter TA, Baron J-C, Mapping the involvement of BA 4a and 4p during Motor Imagery, Neuroimage 41, 92–99 (2008). [PubMed: 18358742]

25. Fuchs X, Bekrater-Bodmann R, Flor H, in Pain, Emotion and Cognition: A Complex Nexus, Pickering G, Gibson S, Eds. (Springer International Publishing, Cham, 2015), pp. 189–207.
26. Di Pino G, Guglielmelli E, Rossini PM, Neuroplasticity in amputees: Main implications on bidirectional interfacing of cybernetic hand prostheses, Progress in Neurobiology 88, 114–126 (2009). [PubMed: 19482228]
27. Herr HM, Riso RR, Song KW, Casler RJ Jr., Carty MJ, Peripheral Neural Interface Via Nerve Regeneration to Distal Tissues (2016) (available at http://www.freepatentsonline.com/y2016/0346099.html).
28. US20190021883 Method And System For Providing Proprioceptive Feedback And Functionality Mitigating Limb Pathology (available at https://patentscope.wipo.int/search/en/detail.jsf;jsessionid=A1589CE54341CFFC8B9A5C5771D109AC.wapp2nA?docId=US236451093&recNum=2031&office=&queryString=&prevFilter=&sortOption=Pub+Date+Desc&maxRec=73603093).
29. Clites TR, Carty M, Srinivasan S, Zorzos A, Herr H, A murine model of a novel surgical architecture for proprioceptive muscle feedback and its potential application to control of advanced limb prostheses, J. Neural Eng. (2017), doi:10.1088/1741-2552/aa614b.
30. Clites TR, Carty MJ, Ullauri JB, Carney ME, Mooney LM, Duval J-F, Srinivasan SS, Herr HM, Proprioception from a neurally controlled lower-extremity prosthesis, Science Translational Medicine 10, eaap8373 (2018). [PubMed: 29848665]
31. Srinivasan SS, Diaz M, Carty M, Herr HM, Towards functional restoration for persons with limb amputation: A dual-stage implementation of regenerative agonist-antagonist myoneural interfaces, Scientific Reports 9, 1981 (2019). [PubMed: 30760764]
32. Clites TR, Herr HM, Srinivasan SS, Zorzos AN, Carty MJ, The Ewing Amputation: The First Human Implementation of the Agonist-Antagonist Myoneural Interface, Plastic and Reconstructive Surgery – Global Open 6, e1997 (2018). [PubMed: 30881798]
33. Clites TR, Carty MJ, Srinivasan SS, Talbot SG, Brånemark R, Herr HM, Caprine Models of the Agonist-Antagonist Myoneural Interface Implemented at the Above- and Below-Knee Amputation Levels, Plast. Reconstr. Surg. 144, 218e–229e (2019).
34. Geyer S, Schormann T, Mohlberg H, Zilles K, Areas 3a, 3b, and 1 of Human Primary Somatosensory Cortex: 2. Spatial Normalization to Standard Anatomical Space, NeuroImage 11, 684–696 (2000). [PubMed: 10860796]
35. Raffin E, Mattout J, Reilly KT, Giraux P, Disentangling motor execution from motor imagery with the phantom limb, Brain 135, 582–595 (2012). [PubMed: 22345089]
36. Guillot A, Collet C, The Neurophysiological Foundations of Mental and Motor Imagery (OUP Oxford, 2010).
37. Motor Units and Muscle Receptors (Section 3, Chapter 1) Neuroscience Online: An Electronic Textbook for the Neurosciences | Department of Neurobiology and Anatomy - The University of Texas Medical School at Houston (available at https://nba.uth.tmc.edu/neuroscience/m/s3/chapter01.html).
38. Confalonieri L, Pagnoni G, Barsalou LW, Rajendra J, Eickhoff SB, Butler AJ, Brain Activation in Primary Motor and Somatosensory Cortices during Motor Imagery Correlates with Motor Imagery Ability in Stroke PatientsInternational Scholarly Research Notices (2012), doi:10.5402/2012/613595.
39. Motor Imagery After Subcortical Stroke | Stroke (available at https://www.ahajournals.org/doi/10.1161/STROKEAHA.108.525766).
40. Pawela CP, Biswal BB, Hudetz AG, Li R, Jones SR, Cho YR, Matloub HS, Hyde JS, Interhemispheric neuroplasticity following limb deafferentation detected by resting-state functional connectivity magnetic resonance imaging (fcMRI) and functional magnetic resonance imaging (fMRI), Neuroimage 49, 2467–2478 (2010). [PubMed: 19796693]
41. Bonini F, Burle B, Liégeois-Chauvel C, Régis J, Chauvel P, Vidal F, Action Monitoring and Medial Frontal Cortex: Leading Role of Supplementary Motor Area, Science 343, 888–891 (2014). [PubMed: 24558161]
42. Szczepanski SM, Knight RT, Insights into Human Behavior from Lesions to the Prefrontal Cortex, Neuron 83, 1002–1018 (2014). [PubMed: 25175878]

43. Kooijman CM, Dijkstra PU, Geertzen JH, Elzinga A, van der Schans CP, Phantom pain and phantom sensations in upper limb amputees: an epidemiological study, Pain 87, 33–41 (2000). [PubMed: 10863043]
44. Xu X, Yuan H, Lei X, Activation and Connectivity within the Default Mode Network Contribute Independently to Future-Oriented Thought, Scientific Reports 6, 1–10 (2016). [PubMed: 28442746]
45. Fischl B, Dale AM, Measuring the thickness of the human cerebral cortex from magnetic resonance images, Proc. Natl. Acad. Sci. U.S.A. 97, 11050–11055 (2000). [PubMed: 10984517]
46. Park JE, Apraxia: Review and Update, J Clin Neurol 13, 317–324 (2017). [PubMed: 29057628]
47. Hernandez-Castillo CR, Galvez V, Mercadillo RE, Díaz R, Yescas P, Martinez L, Ochoa A, Velazquez-Perez L, Fernandez-Ruiz J, Functional connectivity changes related to cognitive and motor performance in spinocerebellar ataxia type 2, Movement Disorders 30, 1391–1399 (2015). [PubMed: 26256273]
48. Westlake KP, Nagarajan SS, Functional Connectivity in Relation to Motor Performance and Recovery After Stroke, Front. Syst. Neurosci 5 (2011), doi:10.3389/fnsys.2011.00008. [PubMed: 21369350]
49. Bollaert RE, Poe K, Hubbard EA, Motl RW, Pilutti LA, Johnson CL, Sutton BP, Associations of functional connectivity and walking performance in multiple sclerosis, Neuropsychologia 117, 8–12 (2018). [PubMed: 29750986]
50. Preiβler S, Dietrich C, Blume KR, Hofmann GO, Miltner WHR, Weiss T, Plasticity in the Visual System is Associated with Prosthesis Use in Phantom Limb Pain, Front Hum Neurosci 7 (2013), doi:10.3389/fnhum.2013.00311. [PubMed: 23372547]
51. Nico D, Daprati E, Rigal F, Parsons L, Sirigu A, Left and right hand recognition in upper limb amputees, Brain 127, 120–132 (2004). [PubMed: 14607796]
52. Imaizumi S, Asai T, Kanayama N, Kawamura M, Koyama S, Agency over a phantom limb and electromyographic activity on the stump depend on visuomotor synchrony: a case study, Front. Hum. Neurosci 8 (2014), doi:10.3389/fnhum.2014.00545. [PubMed: 24478674]
53. Herr HM, Clites TR, Srinivasan S, Talbot SG, Dumanian GA, Cederna PS, Carty MJ, Reinventing Extremity Amputation in the Era of Functional Limb Restoration, Annals of Surgery Publish Ahead of Print (2020), doi:10.1097/SLA.0000000000003895.
54. Hashim E, Rowley CD, Grad S, Bock NA, Patterns of myeloarchitecture in lower limb amputees: an MRI study, Front. Neurosci 9 (2015), doi:10.3389/fnins.2015.00015. [PubMed: 25688184]
55. Yu XJ, He HJ, Zhang QW, Zhao F, Zee CS, Zhang SZ, Gong XY, Somatotopic reorganization of hand representation in bilateral arm amputees with or without special foot movement skill, Brain Research 1546, 9–17 (2014). [PubMed: 24373804]
56. Turner JA, Lee JS, Schandler SL, Cohen MJ, An fMRI Investigation of Hand Representation in Paraplegic Humans, Neurorehabilitation and Neural Repair (2016), doi:10.1177/0888439002250443.
57. Dettmers C, Adler T, Rzanny R, van Schayck R, Gaser C, Weiss T, Miltner WH, Brückner L, Weiller C, Increased excitability in the primary motor cortex and supplementary motor area in patients with phantom limb pain after upper limb amputation, Neuroscience Letters 307, 109–112 (2001). [PubMed: 11427312]
58. Keil B, Blau JN, Biber S, Hoecht P, Tountcheva V, Setsompop K, Triantafyllou C, Wald LL, A 64-channel 3T array coil for accelerated brain MRI, Magn Reson Med 70, 248–258 (2013). [PubMed: 22851312]
59. FreeSurfer (available at https://surfer.nmr.mgh.harvard.edu/).
60. Gratton C, Laumann TO, Nielsen AN, Greene DJ, Gordon EM, Gilmore AW, Nelson SM, Coalson RS, Snyder AZ, Schlaggar BL, Dosenbach NUF, Petersen SE, Functional Brain Networks Are Dominated by Stable Group and Individual Factors, Not Cognitive or Daily Variation, Neuron 98, 439–452.e5 (2018). [PubMed: 29673485]
61. Atlases - FslWiki (available at https://fsl.fmrib.ox.ac.uk/fsl/fslwiki/Atlases).
62. AAL / AAL2 / AAL3 – Neurofunctional Imaging Group (GIN-IMN) (available at http://www.gin.cnrs.fr/en/tools/aal/).

63. Rolls ET, Joliot M, Tzourio-Mazoyer N, Implementation of a new parcellation of the orbitofrontal cortex in the automated anatomical labeling atlas, NeuroImage 122, 1–5 (2015). [PubMed: 26241684]

64. Smith SM, Andersson J, Auerbach EJ, Beckmann CF, Bijsterbosch J, Douaud G, Duff E, Feinberg DA, Griffanti L, Harms MP, Kelly M, Laumann T, Miller KL, Moeller S, Petersen S, Power J, Salimi-Khorshidi G, Snyder AZ, Vu A, Woolrich MW, Xu J, Yacoub E, Ugurbil K, Van Essen D, Glasser MF, Resting-state fMRI in the Human Connectome Project, Neuroimage 80, 144–168 (2013). [PubMed: 23702415]

65. inm7/jubrain-anatomy-toolbox (Institute of Neuroscience and Medicine Brain and Behaviour (INM-7), 2019; https://github.com/inm7/jubrain-anatomy-toolbox).

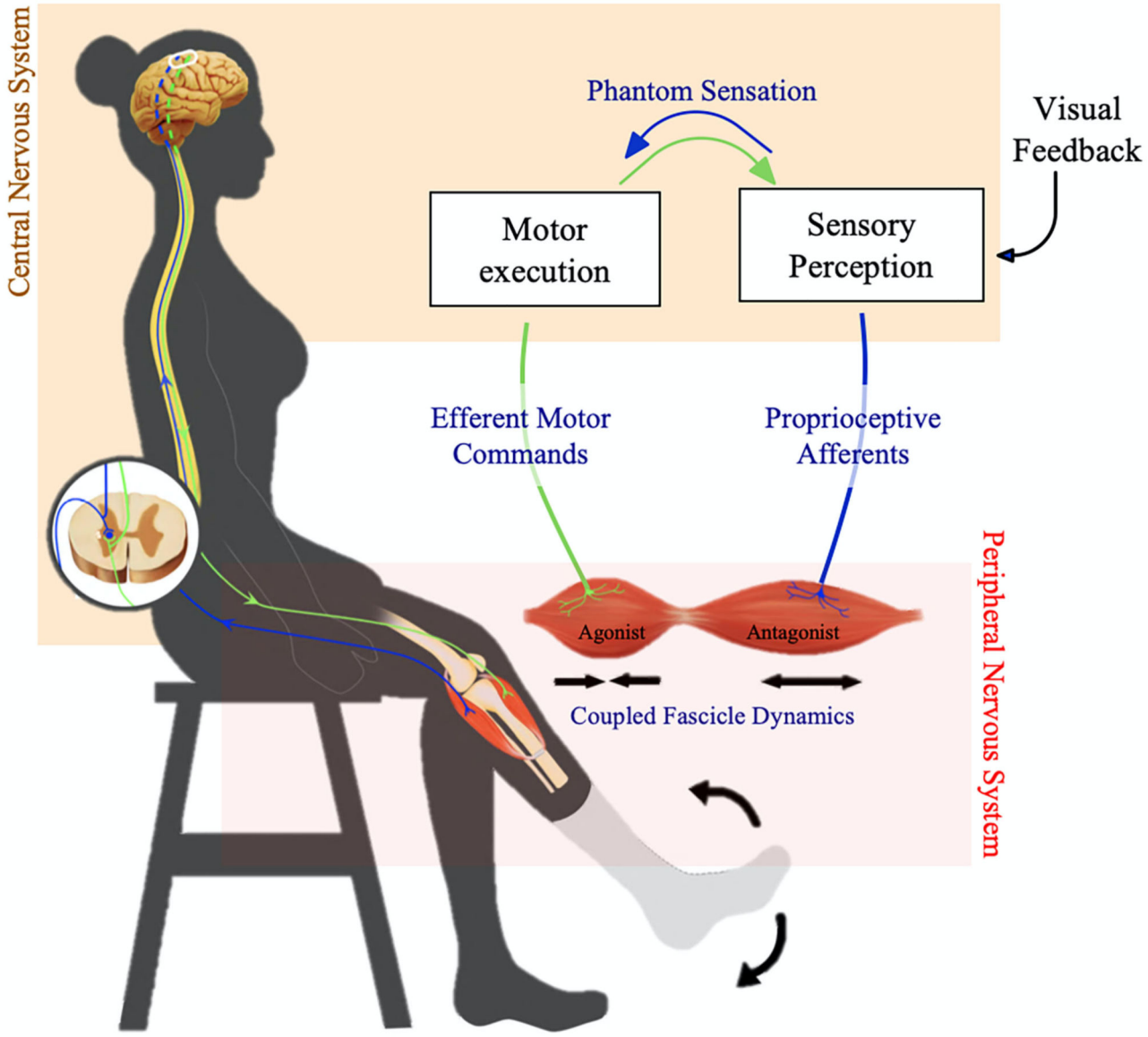

Fig. 1. Amputation architecture and efferent-afferent signaling mechanism.

Schematic of the agonist-antagonist myoneural interface (AMI), a neural prosthetic interface that involves surgically coapting an agonist-antagonist muscle pair to preserve physiological agonist-antagonist muscle dynamics and muscle-tendon proprioceptive afferent signaling, in an individual with lower limb amputation. In the AMI surgical framework, a single AMI, or muscle pair, is created for each biological joint that is to be amputated for which an improved phantom awareness and prosthetic controllability is ultimately sought. This study investigated the link between the AMI amputation and central neuroplasticity in the areas of motor execution and sensory perception through an examination of efferent motor commands (shown in green; tested by EMG during motor control tasks), fascicle dynamics (measured by ultrasound), proprioceptive afferents (measured by functional magnetic resonance imaging), and phantom sensation (shown in blue; measured by psychometric

survey). Encircled in black is the depiction of afferent and efferent pathways from the peripheral nervous system synapsing with the central nervous system.

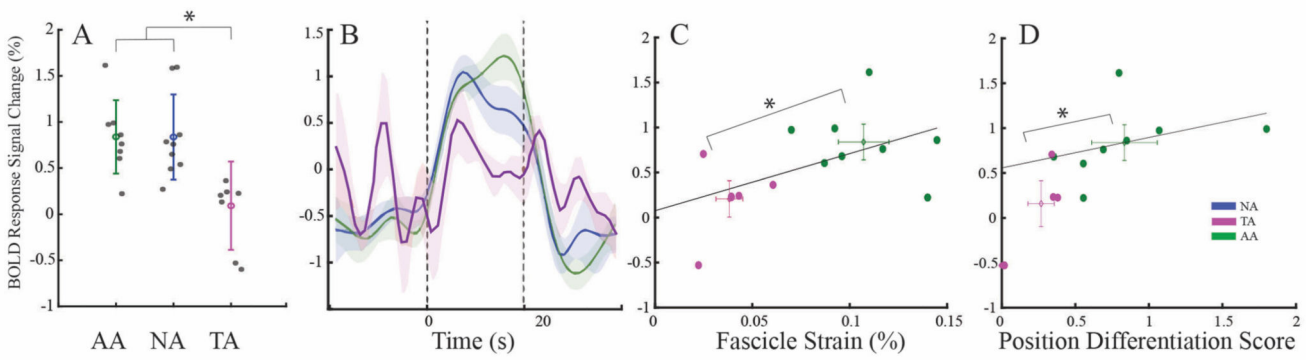

Fig. 2. Functional Activation of ROI in Proprioceptive Center BA3a.

(A) BOLD response of BA3a in the AA, NA, and TA groups. AA and NA, P < 0.63; TA, P < 0.005, Kruskal Wallis. **(B)** Time course of the signal change in BOLD response in BA3a during the task, averaged by group. **(C)** Correlation of the BA3a BOLD response to the fascicle strain from the tibialis anterior (r = 0.66) during cycles of dorsi- and plantarflexion. **(D)** Correlation of the BA3a BOLD response to the score of a position differentiation task, requiring proprioception (r = 0.64). For plots in C and D, the cross bars represent the mean and standard deviation of each group and AA and TA groups cluster distinctly in both (*P < 0.005 MANOVA).

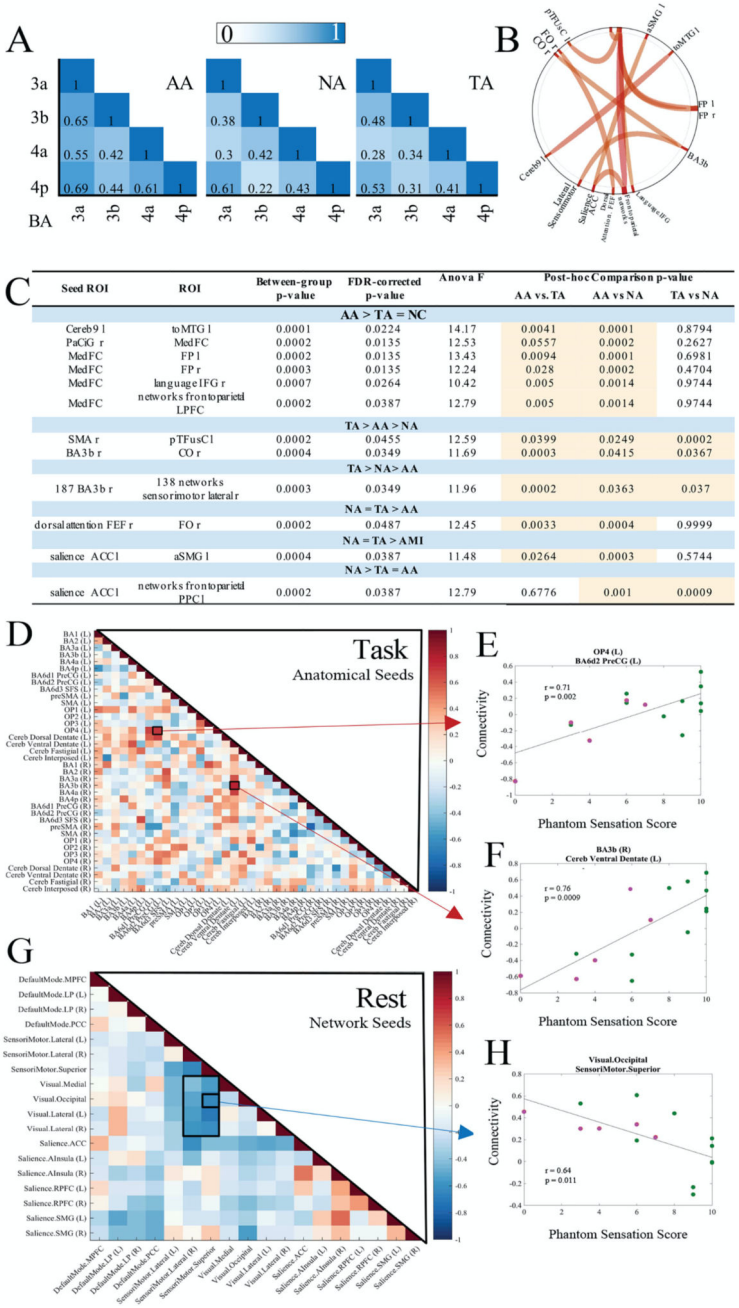

Fig. 3. Functional Sensorimotor Connectivity.

(A) Sensorimotor functional connectivity of the BA 3a, 3b, 4a, and 4p regions within the ankle ROI is represented by averaged Pearson's correlation coefficients. **(B)** ROI-to-ROI functional connectivity across all groups. **(C)** Table of ROI-to-ROI functional connectivities of significance ($p^{FDR} < 0.05$, two-tailed). Post hoc ANOVA analyses presented in the table demonstrate the relative strength of each relationship between groups. Significant comparisons are highlighted in orange. **(D)** Anatomical seed-based cross-ROI correlation to phantom sensation score during task. **(E,F)** The two highest positively ($P < 0.002$, $P <$

0.0009) correlated relationships (OP4/BA6d2 PreCG and BA3b/Cereb ventral dentate) are plotted to demonstrate the distribution of data on a per-individual basis (AA, green, n = 10 and TA, orange, n = 5). **(G)** Network seed-based cross-ROI correlation to phantom sensation score during resting state. **(H)** The strongest negatively correlated relationship ($P < 0.011$) from resting state (visual.occipital/sensorimotor.superior) is plotted to demonstrate the distribution of data on a per-individual basis (AA, green, n = 10 and TA, orange, n = 5).